Analyst

RSC Publishing

PAPER

View Article Online
View Journal | View Issue

Published on 28 March 2013. Downloaded by Michigan State University on 19/01/2016 21:04:23.

Cite this: *Analyst*, 2013, **138**, 3238

Real time monitoring of junction ribonuclease activity of RNase H using chimeric molecular beacons

Bin Liu,* Dan Xiang, Ying Long and Chunyi Tong

Received 1st October 2012
Accepted 28th March 2013

DOI: 10.1039/c3an36414c

www.rsc.org/analyst

As a highly conserved damage repair protein, except for hydrolysis of DNA–RNA heteroduplex endonucleolytically, RNase H can cleave RNA–DNA junctions in Okazaki fragment processing through its junction ribonuclease (JRNase) activity. We report here a real time fluorescence method for detecting JRNase activity of RNase H with high accuracy by applying chimeric molecular beacons as substrates. The detection limit of *E. coli* RNase H is 0.5 U ml^{-1}. The K_m and k_{cat} are 20 nM and 0.6 s^{-1}, respectively. In addition, we used the method to investigate the effect of chemical drugs on the enzyme and found that both penicillin and streptomycin sulfate inhibit its activity with the IC_{50} values of 0.2 and 0.07 mM, respectively. Finally, we applied the method to reliably detect the JRNase level in tumor cells. In summary, these data indicate that the simple, rapid and sensitive method can be hopefully applied for high-throughput detection of samples and drug screening *in vitro*.

Introduction

Enzymes with RNase H activities, which can specifically hydrolyze the RNA strand of the RNA–DNA duplex through an endonucleolytic mechanism, have been identified in many sources, including *E. coli*,[1] yeast,[2] trypanosomes,[3] calf thymus and other cells.[4,5] Recently, RNases H have been suggested to meanwhile possess junction ribonuclease (JRNase) activity that can aid in recognizing the transition from RNA to DNA of an RNA–DNA/DNA hybrid, such as an Okazaki fragment, and cleave it, leaving a mono-ribonucleotide at the 5′ terminus of the RNA–DNA junction.[6–11] In addition to its important role in several cellular processes including DNA replication[2] and DNA repair,[12,13] RNase H is also tightly associated with the retroviral reverse transcription process and drug resistance.[1,14–16] More importantly, it can be used as a tool enzyme in molecular biology and biotechnology, *e.g.* DNA detection,[17,18] removal of mRNA from an mRNA:cDNA duplex, RNA isotope labeling and specific cleavage of RNA in synthetic DNA.[19,20] Until now, the active site and key structural elements necessary for RNA hydrolysis have been recognized through structural analysis of RNase H,[21–27] while biochemical evidence for the function of JRNase is still much limited. In order to explore the mechanism of junction cleavage reaction, developing simple and efficient methods for JRNase activity assay of RNase H still remains to be done.

A number of traditional methods have been used to assay RNase H activities and evaluate the kinetic parameters, through gel electrophoresis,[4,6,7,10] capillary electrophoresis,[28] HPLC,[24] *etc.* Most of them have utilized radio-labeled substrates in conjunction with electrophoresis separation, which are not suitable for large-scale sample analysis. At the same time, all of these methods are indirect, discontinuous, and time-consuming. Furthermore, the HPLC method needs micromolar concentrations of the substrate. Recently, several fluorescence methods, which can efficiently overcome the drawbacks of these traditional methods, have been developed and applied for high throughput activity assay and inhibitor screening.[29–33] However, nearly most of these methods have focused on the nonspecific hydrolysis activity of RNase H and no continuous fluorescence method for monitoring RNA junction cleavage has been reported until now. Therefore, new methods with good sensitivity, simplicity and economy are still in demand. Recent evidence has indicated that due to its JRNase activity RNase H can recognize different aspects of the substrate structure than conventional hybrid duplexes.[6–11] Among them, calf RNase H can cleave RNA–DNA junctions with or without the presence of duplex structures,[6] while *E. coli* JRNase can work on Okazaki fragment-like substrates with base pairing around the DNA–RNA junction.[9] As molecular beacons contain duplex and single-strand oligonucleotides, they can fulfill the structure requirement as JRNase substrates. Based on these results, we designed a class of chimeric molecular beacons and applied them for JRNase activity assay of *E. coli* RNase H in real time.

Materials and methods

All molecular beacons and oligonucleotide strands (Table 1) were synthesized by Takara Biotechnology Co. Ltd (Dalian, China). *E. coli* RNase H possessing JRNase activity was

College of Biology, Hunan University, Changsha, Hunan, 410082, People's Republic of China. E-mail: binliu2001@hotmail.com; Fax: +86 731 88821385; Tel: +86 731 88821385

This journal is © The Royal Society of Chemistry 2013

Published on 28 March 2013. Downloaded by Michigan State University on 19/01/2016 21:04:23.

Table 1 Oligonucleotide strands with different sequences

CMB1	5′-TAMRA-CGCTGCGGCCTCGGr(CACT)GCGTTCGAGCAGCG-DABCYL-3′
CMB2	5′-TAMRA-CGCTGCGGCCTCGr(GCACTG)CGTTCGAGCAGCG-DABCYL-3′
CMB3	5′-TAMRA-CGCTGCGGCCTCr(GGCACTGC)GTTCGAGCAGCG-DABCYL-3′
CMB4	5′-TAMRA-CGCTGCGGCCTr(CGGCACTGCG)TTCGAGCAGCG-DABCYL-3′
CMB5	5′-TAMRA-CGCTGCGGCCr(TCGGCACTGCGT)TCGAGCAGCG-DABCYL-3′
MB (control)	5-TAMRA-CGCTGCTTCAACACCCGCCTCTCCCGGCAGCG-DA BCYL-3
cDNA	5′-TCGAACGCAGTGCCGAGGCC-3′

purchased from Takakra. A 1× reaction buffer [75 mM KCl, 50 mM Tris–HCl, 3 mM $MgCl_2$, 1 mM dithiothreitol, pH 8.3] was used in all reactions unless otherwise indicated. All chemicals were purchased from Sigma-Aldrich.

Fluorescence measurement

All experiments were conducted in a 500 μl quartz cell at 37 °C on a Hitachi FL-2500 spectrofluorometer (λ_{ex} = 521 nm, λ_{em} = 578 nm). Excitation and emission slit widths were 5 nm and 10 nm. Background intensity of the solution was monitored until it remained stable. Then, RNase H or cell-free extracts were added and the subsequent change in fluorescence was recorded as a function of time. The emission spectra were measured by exciting the samples at 521 nm and scanning the emission between 550 and 650 nm. Fluorescence emission intensities were measured at 578 nm.

Real time monitoring of junction cleavage

In a standard 100 μl reaction, 100 nM different kinds of molecular beacons were separately mixed with a buffer containing 75 mM KCl, 50 mM Tris–HCl, 3 mM $MgCl_2$, 10 mM DTT and then incubated for 10 min at 37 °C on the spectrofluorometer. Fluorescence–time curves were recorded after addition of the different amounts of RNase H.

JRNase activity assay

The commercially provided RNase H was diluted with storage buffer (50% glycerol, 20 mM Tris–HCl (pH 7.5), 30 mM NaCl, 0.5 mM EDTA, 1 mM DTT) at 4 °C. In a standard 100 μl reaction, 100 nM CMB5 was mixed with 1× reaction buffer. The mixture was incubated on the spectrofluorometer for 10 min at 37 °C and fluorescence–time curves were recorded after the addition of various concentrations of RNase H and stirring for 4 s.

Kinetics study

Kinetics study of RNase H was performed at 37 °C in 100 μl of the standard solution containing 25–400 nM CMB5. Initial rates were determined by considering only those linear portions (in the first 20 s) of fluorescence curves that yielded <5% of substrate cleavage. Initial rates in units of fluorescence intensity per second were converted to moles per liter per second by dividing by the maximum change in fluorescence intensity and multiplying by the initial substrate concentration. The maximum change in fluorescence intensity for each substrate concentration was obtained by incubation with a large excess of the enzyme under testing. Values of k_{cat}/K_m were calculated from the equation $k_{cat}/K_m = V_0/[E][S]$ by measuring the initial rates at different substrate concentrations.

Inhibitor screening

For the inhibition assay, a total volume of 100 μl standard solution that contained 100 nM CMB5 and various amounts of the drug (penicillin or streptomycin sulfate) were initially incubated at 37 °C for 10 min in a 500 μl quartz cuvette. Then, fluorescence–time curves were monitored immediately at the same temperature after 1 μl RNase H (5 U) was added. Initial velocities were calculated from the data obtained in the first 20 s of time curves. Effects of drugs on RNase H were evaluated from initial velocity variation.

JRNase assay in cell-free extracts

Huh 7 and HCC20986 tumor cells were cultured in DMEM medium and cell-free extracts were prepared as follows: 1×10^6 cells were harvested by trypsin treatment and centrifuged at 1500*g* for 2 min. Cells were washed 3 times with 10 ml of cold PBS, centrifuged and resuspended in 0.5 ml of ice-cold cell lysis buffer (cell signaling) on ice for 5 min. Cells were pulse-sonicated on ice 5 times for 5 s each. Then, centrifuged extracts at 15 000*g* for 20 min at 4 °C and supernatants were collected. The concentration of cell-free extracts was quantitated by measuring the absorbance at 595 nm using Coomassie blue protein reagent (Pierce, Rockford, USA).

Results and discussion

Design and preparation of chimeric DNA–r(N_S)–DNA molecular beacons (CMBs)

Comparing with the isotope labeling method for RNase H assay, new methods based on fluorescence substrates showed significant advantages due to their simplicity and continuity. Among them, molecular beacons are the most widely used probes due to their convenience, stability and high sensitivity.[34] Several methods have been developed for the assay of hydrolytic activity of RNase H by applying the stem of molecular beacons as active sites.[35,36] Similarly, in order to detect JRNase activity of RNase H sensitively, we designed another kind of chimeric molecular beacon, which contains an RNA fragment in the loop with the 5′ end labeled with TAMRA and the 3′ end labeled with DABCYL, as a fluorogenic substrate and report probe (Table 1). The melting temperature of the substrate is predicted to be higher than 60 °C, a value high enough to ensure good stability of the secondary structure at the assay temperature (37 °C). Upon cleavage, the resulting TAMRA-labeled oligonucleotide is expected to dissociate readily from the partly complementary strand, producing a large increase in fluorescence (Fig. 1).

Published on 28 March 2013. Downloaded by Michigan State University on 19/01/2016 21:04:23.

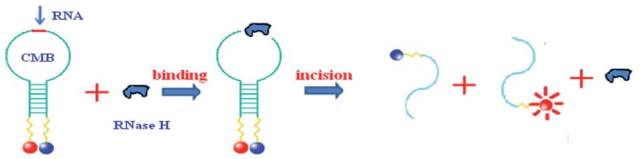

Fig. 1 Structure of the DNA–RNA–DNA chimeric molecular beacon and the strategy employed to quantify JRNase activity of RNase H. The fluorophore (TAMRA) and the quencher (DABCYL) are in close proximity to the intact substrate. Hence, the fluorescence of TAMRA is quenched by DABCYL. Upon RNA cleavage of the loop, the fluorophore is liberated from the hybrid, resulting in a large increase in fluorescence.

On the basis of these theoretical considerations, stem-loop oligonucleotides were synthesized and purified.

E. coli JRNase activity assay

As the first step in the evaluation of the newly prepared substrate, an aliquot of it was excited at 521 nm and an emission spectrum was recorded. The binding process between RNase H and the substrate has been considered to be the initial step in junction cleavage. As protein binding may disturb the original conformation of the probe and cause fluorescence enhancement,[37] control experiments are necessary to determine whether the fluorescence restoration of the probe occurs at this step. From time-scan curves, it can be seen that the fluorescence of the sample containing CMB5 rapidly increases after the addition of RNase H, while the signal of the sample remains at a stable background level when the CMB5 probe is replaced by the MB without an RNA fragment (Fig. 2A). The result indicates that the presence of RNase H in solution cannot disrupt molecular beacon's hairpin conformation through binging step. Subsequently, we investigated the signal to background ratio of the probe and found that the emission of solely CMB5 at 578 nm is very weak, suggesting that the DABCYL group is able to efficiently quench the fluorescence of the TAMRA moiety. However, complete cleavage of the substrate with an excess of *E. coli* RNase H produces a large fluorescence enhancement, with an emission signal at 578 nm that is 30-fold higher than that of the intact probe (Fig. 2B). The result indicates that the CMB probe is suitable to assay JRNase activity of RNase H sensitively.

It has been reported that the length of the RNA fragment can significantly influence RNase H activity on hybrid hydrolysis.[35] In order to get an optimal substrate for RNase H for its JRNase activity so as to increase the method's sensitivity, we investigated the initial velocity change (the fluorescence change in the first 20 seconds) of the reaction caused by the variation of RNA length and found that the fluorescence signal in samples containing various chimeric beacons (CMB1–CMB5) increased after RNase H was added. Interestingly, one sees an increased rate of cleavage as the length of RNA increases. Among the chimeric beacons (CMB1–CMB5) tested, CMB5 containing 12 RNA residues in the loop yields the highest rate for the enzymatic activity (Fig. 3). The difference in the requirement of the RNA fragment length between hydrolysis and JRNase activity of RNase H further confirmed the discrimination of the two kinds of reactions on the other side.[9]

We optimized another important factor, pH value, which can significantly influence RNase H activity.[35,36] The result demonstrates that the activity profile is bell-shaped with a maximum at pH 9.0. Activity of JRNase increases with the increase of pH value from pH 5 and 9, and then slowly decreases from pH 9.0. It still remains at a high level when the pH value reaches 10 (Fig. 4). This profile is very different from the one obtained with poly(rA):poly(rU), which is also bell-shaped with an activity maximum between pH 7 and 7.5.[35] This result shows that RNase H is suited to perform its junction activity above physiological pH condition.

We further investigated the influence of RNase H concentration on the initial velocity under the optimal conditions by applying CMB5 as a substrate. Time curves of fluorescence are illustrated in Fig. 5. The result shows that the initial velocity becomes faster as the enzyme concentration gradually increased. Along with the lapse of time, the removal velocity slows down gradually with the diminishing of the reactant MB5 probe. In the range from 1 to 80 U ml^{-1}, the initial velocity is directly proportional to the enzyme concentration. This

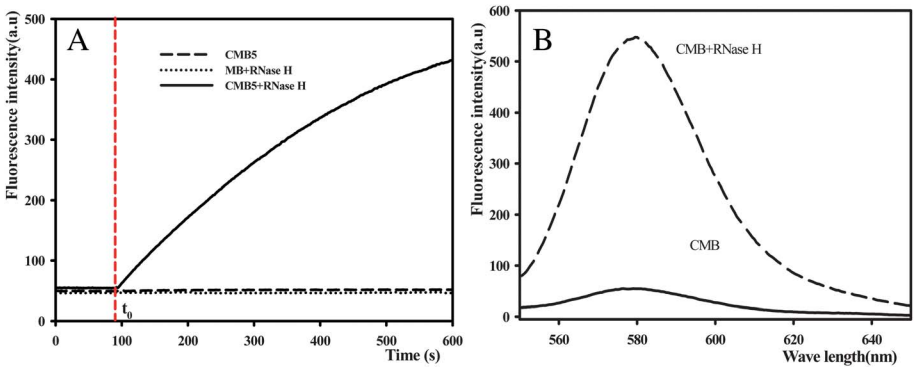

Fig. 2 (A) Time curves of fluorescence intensity. Curves represent the time courses of samples A, B and C. At time t_0, RNase H was added to the sample. (B) Emission spectra of the chimeric molecular beacon and its cleavage product. Spectra of the substrate before (solid line) and after (dashed line) treatment with *E. coli* RNase H were recorded with excitation at 521 nm. Digestion had been performed in 50 mM Tris–HCl (pH 8.3), containing 75 mM KCl, 3 mM $MgCl_2$, 4 mM DTT, 20 μg ml^{-1} BSA, 100 nM substrate and 6 U *E. coli* RNase H, at 37 °C for 15 min.

This journal is © The Royal Society of Chemistry 2013

Published on 28 March 2013. Downloaded by Michigan State University on 19/01/2016 21:04:23.

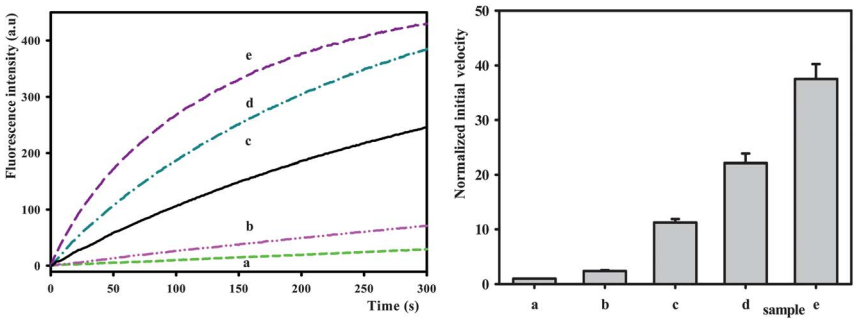

Fig. 3 Fluorescence curves of CMBs digested by *E. coli* RNase H in 1× RNase H buffer. The number of RNA bases from curve a to e is 4, 6, 8, 10 and 12, respectively. [RNase H] = 50 U ml^{-1}, [CMB] = 100 nM.

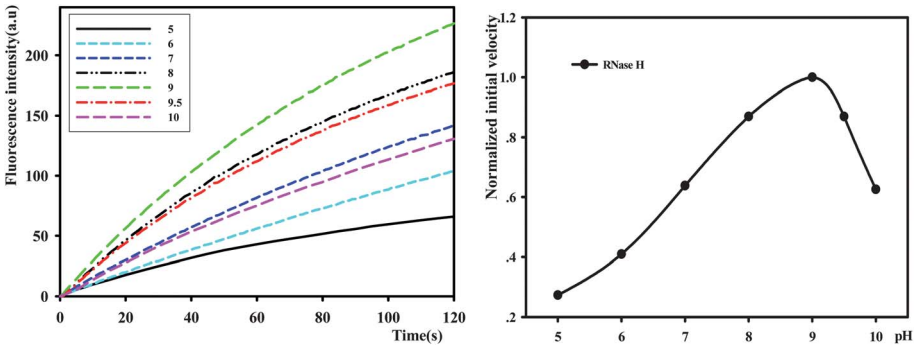

Fig. 4 Fluorescence curves of CMB5 digested by *E. coli* RNase H in 1× reaction buffer under different pH values. [RNase H] = 50 U ml^{-1}, [CMB5] = 100 nM.

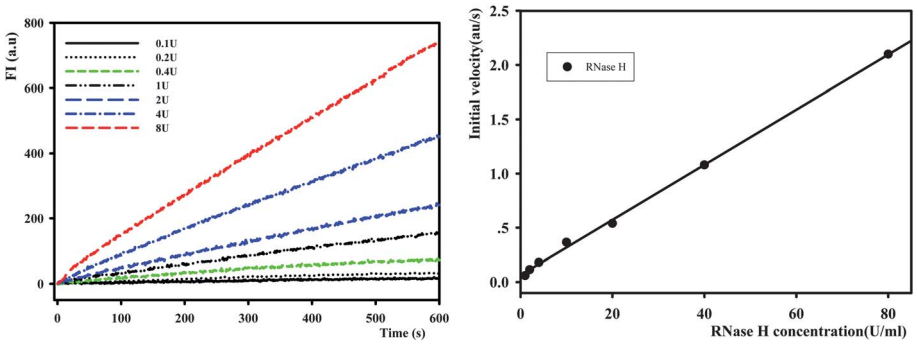

Fig. 5 Substrate cleavage by *E. coli* RNase H. Assays were performed at 37 °C in 50 mM Tris–HCl (pH 8.3), containing 75 mM KCl, 50 mM Tris–HCl, 3 mM $MgCl_2$, 4 mM DTT, 20 μg ml^{-1} BSA and 100 nM CMB5. The fluorescence intensity was measured at 578 nm upon excitation at 521 nm. The left panel shows representative reaction progress curves obtained from 1–80 U ml^{-1} RNase H respectively. The right panel shows the initial rates of substrate cleavage as a function of the concentration of *E. coli* RNase H.

relationship shows that removal kinetics obeys the Michaelis–Menten equation. The detection limit of RNase H assay is 0.5 U ml^{-1} (based on three times higher fluorescence intensity than the background noise). The assay with the advantages of simplicity, rapidity, sensitivity and a wide dynamic range makes itself a useful method for analysis of RNase H activity.

Kinetics of JRNase

An attempt to measure individually the kinetic parameters k_{cat} and K_m of JRNase was performed by testing the enzyme at substrate concentrations between 50 and 400 nM. The initial cleavage velocity, V_0, was measured from the fluorescence change in the first 20 seconds of time curves. Plotting V_0 *versus* 1/[S] yields a straight concentration line (Fig. 6). This indicates that the kinetics data fit well with the Michaelis–Menten equation. From the Lineweaver–Burk plot, the important kinetic parameters, K_m and k_{cat} are determined to be 20 nM and 0.6 s^{-1}, respectively. This implies that the affinity for the substrate of JRNase is similar to that of *E. coli* RNase H, whose K_m values for similar substrates are in the nM range.[35] Nevertheless, the JRNase activity is expected to be highly effective

Published on 28 March 2013. Downloaded by Michigan State University on 19/01/2016 21:04:23.

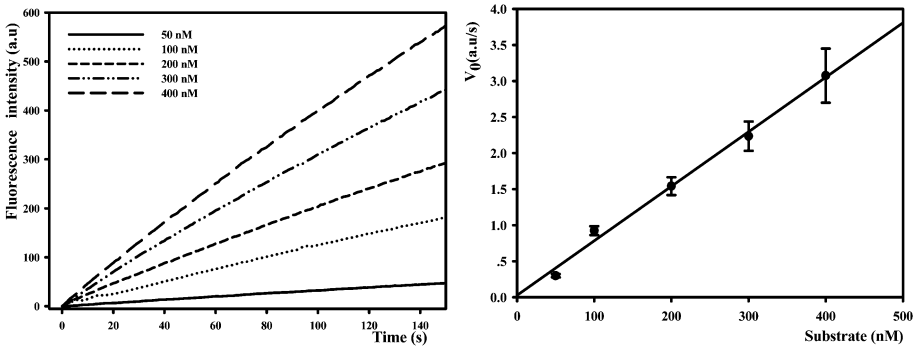

Fig. 6 Michaelis–Menten plot for *E. coli* RNase H. Assays were performed as detailed in Fig. 5. [CMB5] = 20–400 nM, [RNase H] = 50 U ml^{-1}.

even at low substrate concentration due to the relatively high k_{cat}/K_m value (3×10^7 M^{-1} s^{-1}). Since these values were obtained at pH 8.3, the actual K_m values at physiological solution (pH $\sim$ 7.4) should be higher.

Metal ions can differently inhibit JRNase activity

It has been reported that *E. coli* RNase H prefers the Mn^{2+} ion for RNase activity but the Mg^{2+} ion for JRNase activity.[9,38] Calf RNase HI also seems to prefer the Mg^{2+} ion to the Mn^{2+} ion.[6] These results demonstrate that the conformation of the catalytic centre of RNase H protein would change depending on the variety of the metal ion. In order to confirm this point and further explore the relationship between heavy metal ions and JRNase activity of RNase H, we investigated the initial velocity change of the reaction caused by the presence of metal ions. In brief, the substrate was incubated in reaction buffer containing 3 mM $MgCl_2$ with different concentrations of Cd(II), As(III), Cu(II), Hg(II), or Pb(II). After incubation on the spectrophotometer for 10 min, RNase H was added, and the ability of JRNase activity to convert the longer DNA–RNA–DNA strand to shorter oligonucleotide products was evaluated from the initial velocity. We found that all investigated metal ions quantitatively exhibit inhibitory effects on enzyme activity in a concentration-dependent manner (Fig. 7A), while the extent of inhibition varied significantly according to the metal ion type. Using the double reciprocal plot method, IC_{50} (half-maximal inhibitory concentration) values for Cd(II), As(III), Cu(II), Hg(II) or Pb(II) are determined to be 2.86, 1.58, 1.04, 0.87 and 0.78 mg l^{-1}, respectively. Interestingly, our *in vitro* results show that the resistance ability of *E. coli* against heavy metal ions Cd(II), As(III) is much higher than that of Hg(II), similar to that of metal ions against JRNase activity in previous reports.[39–41] These results demonstrate that the method can be hopefully applied for the investigation of resistance ability of metal ions on *E. coli* growth and proliferation. In addition, we also confirmed that the influence of EDTA, which can act as an efficient inhibitor, on RNase H activity (Fig. 7B).

Inhibitor selection of JRNase

Many antiviral drugs are a class of medication used for selectively treating viral infections through inhibiting specific enzyme activity.[15,16] For example, the reverse transcriptase-associated RNase H has become an attractive non-traditional target for anti-viral drug development.[41–43] Until now, new antivirus drugs are in demand, particularly drugs targeted to viral functions which are not inhibited yet by the current treatments. To more broadly assess the applicability of this new method for the anti-JRNase drug screening, we determined the impact of penicillin and streptomycin sulfate, inhibitors of some enzymes at millimolar concentrations,[44–46] as model compounds on

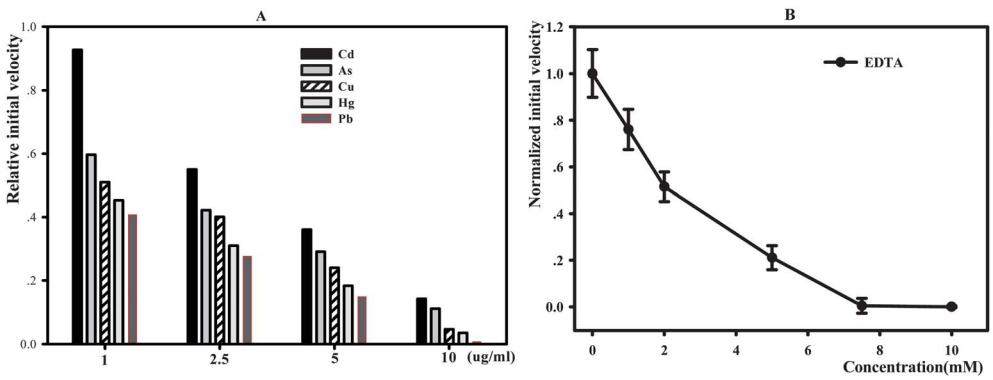

Fig. 7 Effect of metal ions and EDTA on *E. coli* JRNase activity. The initial velocity was monitored in the presence of different factors. Assays were performed as described in Fig. 4. [RNase H] = 50 U ml^{-1}, [CMB5] = 100 nM.

 This journal is © The Royal Society of Chemistry 2013

Published on 28 March 2013. Downloaded by Michigan State University on 19/01/2016 21:04:23.

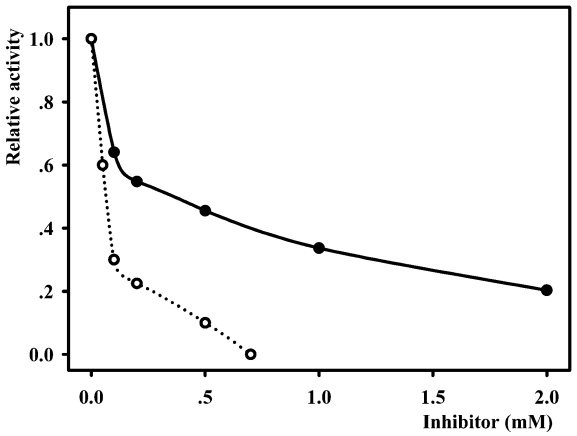

Fig. 8 Inhibition efficiency of *E. coli* JRNase activity by penicillin (filled circles) and streptomycin sulfate (empty circles). IC_{50} values were obtained from curves shown in this figure.

JRNase activity. In the inhibition assay, mixtures of CMB5 and inhibitor were incubated for 10 min, RNase H was then added and the process was monitored for 10 min to allow cleavage. The IC_{50} value (the inhibitor concentration required to reduce enzyme activity by 50%) was obtained from the plot of initial velocity *versus* inhibitor concentration. Both penicillin and streptomycin sulfate were found to inhibit JRNase with IC_{50} values of 0.2 and 0.07 mM, respectively (Fig. 8), the concentrations are in the same order magnitude as those of previous reports.[44–47] These results demonstrate that the simple, rapid and efficient method described herein provides an alternative approach for evaluating inhibitors and drug screening targeted on JRNase active sites.

Assay of JRNase in tumor cell-free extracts

Considering its critical roles in the regulation of important cellular processes,[1,2,13] rapid and accurate detection of JRNase activity in biological samples is of great importance. Though several fluorescent probes as RNase H substrates have been exploited, simple sensors that can rapidly detect JRNase are scarce so far. With a sensitive assay for JRNase activity in hand, we next turned to the analysis of cell-free extracts from different tumor cells. However, we found that cell-free extracts caused fluorescence increase of the MB or CMB solution when the standard buffer was employed. The result, which is consistent with previous reports,[48–50] demonstrates that non-specific digestion of nuclease in extracts can produce false signals and accordingly affect the reliability of the enzyme assay. In order to enhance assay reliability, we added sodium phosphate and carrier nucleic acid including poly(dI:dC), oligo DNA and yeast tRNA to buffer to inhibit nuclease activity as previously described.[48–50] As we expected that the employment of inhibitors can wholly inhibit non-specific nuclease activity in cell-free extracts, we applied the new method to detect the JRNase level in Huh7 and HCC20986 cells. From the result (Fig. 9), we found that the fluorescence intensity of the MB solution containing nuclease inhibitors remained at the background level when 40 μg of HCC20986 or Huh7 cell-free extracts were added, while the fluorescence signal in CMB5 solution containing the same inhibitors increased after the same amount of different cell-free extracts were added (Fig. 9). By comparing the initial velocities, we can conclude that the activity level of RNase H in HCC20986 cells is 2.5 fold higher than that of Huh7 cells. In addition, we designed another experiment to further confirm the reliability of JRNase activity detection. When the same amount of cell-free extracts was added to the CMB5 solution containing nuclease inhibitors and 8 μM streptomycin sulfate (JRNase inhibitor), there was no fluorescence increase observed again (data not shown). These results fully demonstrate that the chimeric molecular beacon can be effectively employed to measure JRNase activity of RNase H in cell-free extracts *in vitro*. The major benefits of the fluorometric assay are improved experimental reproducibility, elimination of radioactivity and a substantial cost reduction when compared to conventional radio-labeled substrates.

Conclusions

In summary, the chimeric molecular beacon for its high signal to noise ratio has found interesting applications in detecting JRNase activity assay. Integrated with the inherited signal-transfer mechanism, the binding and cleaving elements can be used as sensitive probes for enzymatic reaction. This signaling approach has merits for application in activity assay and kinetics analysis for several reasons. First, detection from monitoring the signal change corresponding to conformational change gives a real-time portrayal of what is happening in the

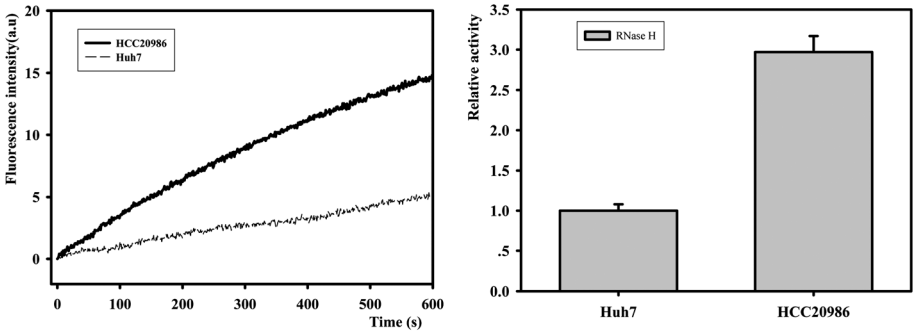

Fig. 9 Detection of JRNase activity of RNase H in tumor cell-free extracts. [CMB5] = 100 nM, the amount of cell-free extracts is 40 μg.

Published on 28 March 2013. Downloaded by Michigan State University on 19/01/2016 21:04:23.

reaction and avoids problems arising from stopping the reaction and taking out samples every few minutes, such as in gel electrophoresis methods. Moreover, as there is no necessity to stop reactions in the middle with inhibitors, it can give a more precise response that can only come from the cleavage activity of the enzyme. Second, shorter detection times are needed. Real-time monitoring avoids any subsequent detection and analysis steps, so it shortens the detection time for each sample and minimizes environmental effects, thereby affording more precise detection. The real-time fluorescence assay we have developed here shows great advantages in these aspects for its simplicity, rapidity, easy construction, and high sensitivity. These properties will enable the construction of chimeric beacons for different types of RNase activity studies *in vitro* and the method, coupled with other expertise, will bring the development of promising drug candidates for clinical trial testing.

Acknowledgements

This work was partially supported by the Fundamental Research Funds for the Central Universities of China (531107040012, 531107040496), the China National Grand Program on Key Infectious Disease (2009ZX10004-312), the National Natural Science Foundation of China (81271885), and the "985" Project fund to Hunan University.

References

1 J. P. Leis, I. Berkower and J. Hurwitz, *Proc. Natl. Acad. Sci. U. S. A.*, 1973, **70**, 2466.
2 T. Ogawa and T. Okazaki, *Mol. Gen. Genet.*, 1984, **193**, 231.
3 K. Katayanagi, M. Miyagawa, M. Matsushima, M. Ishikawa, S. Kanaya, M. Ikehara, T. Matsuzaki and K. Morikawa, *Nature*, 1990, **347**, 306.
4 H. J. Huang, J. N. Liao and S. Cohen, *Nature*, 1998, **391**, 99.
5 H. Mitsuru, N. Eriko, K. Shigenori and R. J. Crouch, *J. Biol. Chem.*, 1997, **272**, 22015.
6 R. S. Murante, L. A. Henricksen and R. A. Bambara, *Proc. Natl. Acad. Sci. U. S. A.*, 1998, **95**, 2244.
7 M. Haruki, Y. Tsunaka, M. Morikawa and S. Kanaya, *FEBS Lett.*, 2002, **531**, 204.
8 N. Ohtani, H. Yanagawa, M. Tomita and M. Itaya, *Biochem. J.*, 2004, **381**, 795.
9 N. Ohtani, M. Tomita and M. Itaya, *FEBS J.*, 2008, **275**, 5444.
10 N. Ohtani, M. Tomita and M. Itaya, *Biochem. J.*, 2008, **412**, 517.
11 M. P. Rychlik, H. Chon, S. M. Cerritelli, P. Klimek, R. J. Crouch and M. Nowotny, *Mol. Cell*, 2010, **40**, 658.
12 D. Bubeck, M. A. Reijns, S. C. Graham, K. R. Astell, E. Y. Jones and A. P. Jackson, *Nucleic Acids Res.*, 2011, **39**, 3652.
13 F. Lazzaro, D. Novarina, F. Amara, D. L. Watt, J. E. Stone, V. Costanzo, P. M. Burgers, T. A. Kunkel, P. Plevani and M. Muzi-Falconi, *Mol. Cell*, 2012, **45**, 99.
14 M. P. Ready, B. J. Katzin and J. D. Robertus, *Proteins: Struct., Funct., Genet.*, 1988, **3**, 53.
15 G. R. Nakayama, P. Bingham, D. Tan and K. A. Maegley, *Anal. Biochem.*, 2006, **351**, 260.
16 K. A. Delviks-Frankenberry, G. N. Nikolenko and V. K. Pathak, *Viruses*, 2010, **2**, 1476.
17 C. Jung, J. W. Chung, U. O. Kim, M. H. Kim and H. G. Park, *Biosens. Bioelectron.*, 2011, **26**, 1953.
18 C. Jung, J. W. Chung, U. O. Kim, M. H. Kim and H. G. Park, *Anal. Chem.*, 2010, **82**, 5937.
19 A. Ogawa, *ChemBioChem*, 2011, **12**, 881.
20 O. Duss, C. Maris, C. Schroetter and F. H. Allain, *Nucleic Acids Res.*, 2010, **38**, e188.
21 V. Pena, A. Rozov, P. Fabrizio, R. Luhrmann and M. C. Wahl, *EMBO J.*, 2008, **27**, 2929.
22 Y. Uchiyama, Y. Miura, H. Inoue, E. Ohtsuka, Y. Ueno, M. Ikehara and S. Iwai, *J. Mol. Biol.*, 1994, **243**, 782.
23 S. T. Crooke, K. M. Lemonidis, L. Neilson, R. Griffey, E. A. Lesnik and B. P. Monia, *Biochem. J.*, 1995, **312**, 599.
24 E. Kanaya and S. Kanaya, *FEBS Lett.*, 1995, **231**, 557.
25 G. L. Beilhartz and M. Gotte, *Viruses*, 2010, **2**, 900.
26 P. S. Pallan and M. Egli, *Cell Cycle*, 2008, **7**, 2562.
27 M. H. Ho, M. De Vivo, M. Dal Peraro and M. L. Klein, *J. Am. Chem. Soc.*, 2010, **132**, 13702.
28 K. C. Chan, S. R. Budihas, S. F. J. Le Grice, M. A. Parniak, R. J. Crouch, S. A. Gaidamakov, H. J. Isaaq, A. Wamiru, J. B. McMahon and J. A. Beutler, *Anal. Biochem.*, 2004, **331**, 296.
29 S. W. Alexander, E. Abbasali, J. D. Masad and H. E. H. Robert, *Nucleic Acids Res.*, 2010, **38**, 1048.
30 M. A. Parniak, K. L. Min, S. R. Budihas, S. F. J. Le Grice and J. A. Beutler, *Anal. Biochem.*, 2003, **322**, 33.
31 G. R. Nakayama, P. Bingham, D. Tan and K. A. Maegley, *Anal. Biochem.*, 2006, **351**, 260.
32 D. Hu, F. Pu, Z. Huang, J. Ren and X. Qu, *Chem.–Eur. J.*, 2010, **16**, 2605.
33 Y. Zhang, Z. Li, Y. Cheng and X. Lv, *Chem. Commun.*, 2009, 3172.
34 S. Tyagi and F. R. Kramer, *Nat. Biotechnol.*, 1996, **14**, 303.
35 J. Rizzo, L. K. Gifford, X. Zhang, A. M. Gewirtz and P. Lu, *Mol. Cell. Probes*, 2002, **16**, 277.
36 Y. Chen, C. J. Yang, Y. Wu, P. Conlon, Y. Kim, H. Lin and W. Tan, *ChemBioChem*, 2008, **9**, 355.
37 Z. Tang, K. Wang, W. Tan, J. Li, L. Liu, Q. Guo, X. Meng, C. Ma and S. Huang, *Nucleic Acids Res.*, 2003, **23**, e148.
38 N. Ohtani, H. Yanagawa, M. Tomita and M. Itaya, *Nucleic Acids Res.*, 2004, **32**, 5809.
39 D. W. Porter, H. Yakushiji, Y. Nakabeppu, M. Sekiguchi, M. J. Fivash Jr and K. S. Kasprzak, *Carcinogenesis*, 1997, **18**, 1785.
40 D. H. Nies, *Appl. Microbiol. Biotechnol.*, 1999, **51**, 730.
41 J. S. Grewal and R. P. Tiwari, *J. Med. Microbiol.*, 1990, **32**, 223.
42 K. Tatyana, E. Francesc, Z. Luca, F. Giovanni, Y. C. Cheng, E. D. Ginger and T. Enzo, *Med. Chem.*, 2009, **5**, 398–410.
43 T. A. Kirschberg, M. Balakrishnan, N. H. Squires, *et al.*, *J. Med. Chem.*, 2009, **52**, 5781.

 This journal is © The Royal Society of Chemistry 2013

44 B. Chandrakala, R. K. Shandil, U. Mehra, S. Ravishankar, P. Kaur, V. Usha, B. Joe and S. M. deSousa, *Antimicrob. Agents Chemother.*, 2004, **48**, 30.
45 B. Ostash and S. Walker, *Curr. Opin. Chem. Biol.*, 2005, **9**, 459.
46 G. Ceriotti, *Nature*, 1949, **163**, 874.
47 A. Mandal and S. K. Majumdar, *Appl. Microbiol.*, 1968, **16**, 1786.
48 C. Wu, *Nature*, 1984, **309**, 229.
49 C. Wu, *Nature*, 1985, **317**, 84.
50 J. K. Wang, T. X. Li, X. Y. Guo and Z. H. Lu, *Nucleic Acids Res.*, 2005, **33**, e23.

Published on 28 March 2013. Downloaded by Michigan State University on 19/01/2016 21:04:23.